

A SIMPLIFIED METHOD OF ENDOSCOPIC IMAGE DISTORTION CORRECTION BASED ON GREY LEVEL REGISTRATION

R. Miranda-Luna, W.C.P.M. Blondel, C. Daul, Y. Hernandez-Mier, R. Posada and D. Wolf

CNRS UMR 7039 – CRAN (Centre de Recherche en Automatique de Nancy)
2, avenue de la Forêt de Haye, 54516 Vandoeuvre-Lès-Nancy Cedex, France.

ABSTRACT

We present a new method of endoscopic camera calibration for non-linear radial distortion correction. The algorithm implemented computes both projective (camera) and polynomial (distortion) transformations. The optimization process registers the corrected distorted pattern image with the non-distorted one. Mutual information was used as measure of similarity and stochastic gradient descent method for optimization.

The algorithm was tested with two b/w (chessboard, concentric circles) and one grey level patterns, for 3 angular positions of the endoscope (0° , 5° and 10° to perpendicular). Convergence time increased with the angle. Maximal mean correction error was less than 0.45 % with optimized distortion parameters calculated for the grey level pattern. Tested inclinations did not have significant effects on errors. Results obtained show the interest of the method proposed that requires only approximative perpendicular positioning of the endoscope and simple grey level calibration patterns without precise geometrical characteristics.

1. INTRODUCTION

Video-based endoscopic systems are viewing inspection tools used in standard clinical examination of inside body cavities and hollow organs. They permit to generate and to record images sequences, each image showing a small part of the fully scanned observed area. Therefore, a unique global image of this area should constitute a simplified and easy to use representation helpful to the clinician in post-operative observations [4]. Bi-dimensional cartographies or high resolution panoramas of the overall surface of the observed tissues can be built by mosaicing these successive overlapping images. The mosaicing process consists firstly in finding the registration parameters of two consecutive images from the sequence and secondly in combining all the registered images to build one panoramic image. To do so, a search space has to be defined. In the case of free distorted acquisition systems, a

projective transformation is a suitable model for the camera and the motion of the viewpoint between images [1,5].

However, endoscopes are instruments designed to have a small diameter examination tube and a distal tip optics allowing image acquisition over a wide field of view (FOV). Such lenses therefore produce non-linear geometrical distortion (not angular but mainly radial) named barrel distortion [2,6], which is a problem for accurate and automatic registration. Furthermore, in clinical practice, several different endoscopes are used and submitted to cleaning (decontamination) processes. This implies systematic recalculation of correction parameters for each endoscope. The correction method should therefore be easy to implement. To perform barrel distortion correction, a calibration step is needed for determining the optical distortion center and the radial distortion parameters. Most recent works on the calculation of correction parameters of endoscopes barrel distortion propose methods based on the acquisition of an image of a calibration grid with precise geometrical characteristics, with or without need of exact perpendicular positioning [1,3]. We propose a more flexible and easy to handle method to determine the coefficients of the non-linear polynomial transformation by registering a non-distorted pattern and the corresponding distorted image acquired with an endoscope. The idea is to determine during the optimisation process of the registration both, the parameters of a projective transformation matrix (extrinsic parameters) and the polynomial coefficients (intrinsic parameters). By this way, neither calibration pattern with precise geometrical characteristics nor precise positioning platform are needed. We present here our method and the results obtained for various types of pattern and for different angular position of the viewpoint.

2. MATERIALS AND METHODS

2.1. Images acquisition and test protocol

The calibration procedure starts with the acquisition of the image of a motionless planar scene characterised by a known reference pattern. Images were acquired through a

FUJINON FG-100FP fibroscope by a b/w CCD camera (Leritier 760 ULL) and digitized using a video board Matrox Meteor-II to obtain an image size of 768 x 576.

By means of a positioning system, the viewpoint (distal tip of the endoscope) was set at a distance between 32 and 39 mm to the scene such that the image pattern filled the whole sensor's FOV. In order to evaluate the influence of perspective on the sensibility of the method to give good correction parameters, positions of the viewpoint were tested with 0°, 5° and 10° angles from the perpendicular to the pattern plane. Furthermore, in order to evaluate the efficiency of the method according to the nature of information contained in images, we tested two black and white patterns with particular shapes (chessboard and concentric circles) and one grey level image (Figure 1). The original non-distorted patterns were images stored in the computer. To reduce the processing time, all images were processed at dimension of 384 by 288 pixels, resulting in a resolution of 163 dpi.

2.2. Distortion correction and perspective models

Non linear radial distortion correction is modelled by the optical center coordinates (C_x, C_y) and a radial distortion r' expressed as the following polynomial relationship :

$$r' = \sum_{i=1}^N k_i \cdot r^i \quad \text{with } k_i=1 \quad (1)$$

where r is the radial distance between an image point of coordinates (x,y) and the optical center, k_i are correction coefficients used to obtain the undistorted image.

The number of parameters k_i to be calculated depends on the importance of the distortion and on the precision required to model it. In our case we choose $N=5$ which was evaluate to be a good compromise between processing time and calculation precision. The model used for the 2D-2D camera-to-scene transformation takes into account translations, rotations, viewpoint and scale factor existing between the original non-distorted image U and the distorted acquired image V :

$$U = TV = T_e T_i V \quad (2)$$

where T_e is a 2D projective matrix of extrinsic parameters and T_i is the intrinsic (polynomial) parameters matrix. Since both transformation (projective and polynomial) are independents, resulting radial corrections parameters (C_x, C_y and k_i) can be isolated after the registration procedure of calibration in order to perform a systematic radial correction of all images acquired with the endoscope as long as its optics will not be modified.

2.3. Registration algorithm and parameters calculation

Our method consists in optimizing extrinsic and radial distortion correction parameters in order to registrate the

corrected distorted image to the original non-distorted pattern. We performed a 2D-2D grey-level image registration method based on mutual information. A stochastic gradient descent algorithm was implemented to optimize the computation of the parameters of both projective and polynomial transformations.

Mutual information $I(U,W)$ is a very robust measure of similarity between superimposed parts of two images U and W characterized only by grey level distributions. In order to obtain a measure less sensitive to problems of poorly informative overlapping areas (like background or no particular anatomical structures) we used the following form of definition including the entropy of each images $H(U)$, $H(W)$ and the joint entropy $H(U,W)$:

$$I(U,W) = H(U) + H(W) - H(U,W) \quad (3)$$

where $W = TV$ corresponds to a corrected distorted image. An iterative global optimisation method of stochastic gradient descent (well adapted to overcome narrow local maximum that can trap gradient techniques) was implemented to determine the parameters values of optimised transformation \tilde{T} leading to the global maximum of the mutual information function such as :

$$\tilde{T} = \arg \max_T (I(U,TV)) \quad (4)$$

Typical polynomial and projective initial parameters were: optical center = image center, $k_i=0$, scale factor = 0.85 and initial translations and rotations = 0. The values of these parameters were updated at each iteration of the algorithm so that :

$$T(i+1) = T(i) + \lambda \frac{\partial I(U, T(i)V)}{\partial T} \quad \text{at } (i+1)^{\text{th}} \text{ step} \quad (5)$$

where λ is a convergence rate parameter that is progressively reduced when approaching the maximum.

Error of radial distortion correction was estimated on the basis of the chessboard pattern (Figure 1) by calculating euclidean distances between centre points of corresponding white squares in the binarized endoscopic image after correction and in the non-distorted image. In order to compare identical types of errors for all patterns, the correction parameters obtained for circles and grey level patterns and for all viewpoint angles were applied to their corresponding distorted chessboard images. The corrected images therefore obtained were used for errors calculation. Final errors e_{mean} and e_{max} were expressed as average and maximum errors normalized to the diameter of the FOV (449 pixels) [1].

3. RESULTS AND DISCUSSION

Figure 1 shows the results of the correction obtained for the three different patterns A, B, C acquired each from three angular positions of the endoscope to the pattern plane (0°, 5° and 10° deviation from perpendicular).

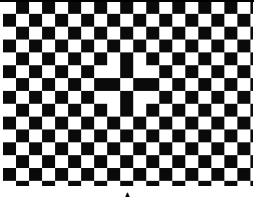
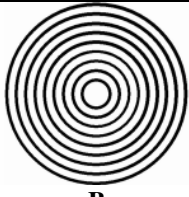

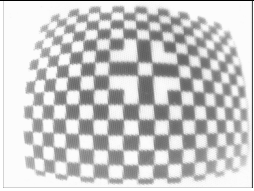
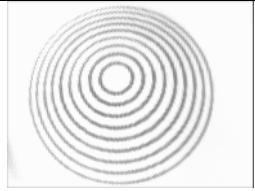

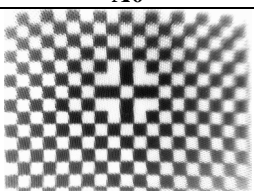
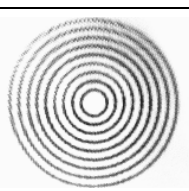
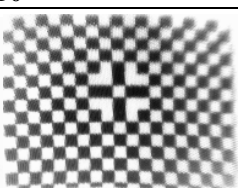

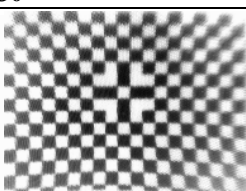
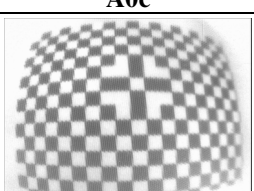
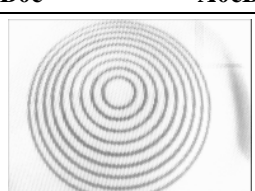

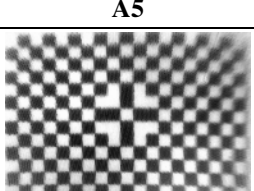
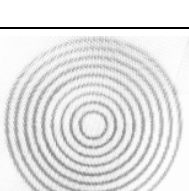



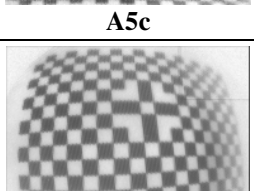
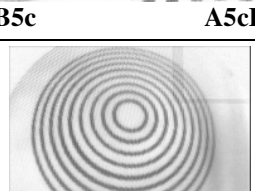
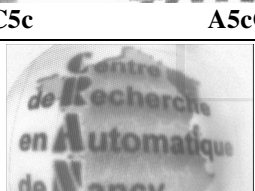
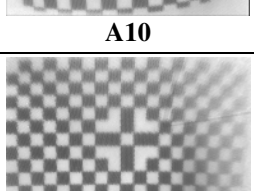
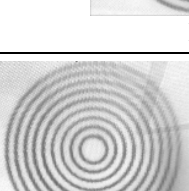
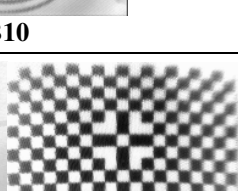

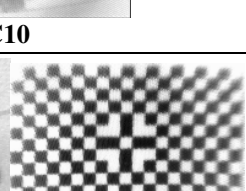
Original images											
	A		B		C						
0° Angle	Acquired										
	Corrected										
		A0c		B0c		A0cB		C0c		A0cC	
5° Angle	Acquired										
	Corrected										
		A5c		B5c		A5cB		C5c		A5cC	
10° Angle	Acquired										
	Corrected										
		A10c		B10c		A10cB		C10c		A10cC	

Figure 1. Visual results for 3 original patterns A, B and C.

A_i, B_i, C_i (i=0,5,10) – Distorted endoscopic images of A, B, C at 0°, 5° and 10° from perpendicular.

A_{ic}, B_{ic}, C_{ic} (i=0,5,10) – Corrected endoscopic images of A, B, C at 0°, 5° and 10° from perpendicular.

A_{icB}, A_{icC} (i=0,5,10) – Corrected images of A based on correction parameters of B, C at 0°, 5° and 10° from perpendicular.

Table 1. Numerical results after optimisation

 k_i and $C_{x,y}$ – Radial distortion correction coefficients (dimensionless) and optical center coordinates (pixels) e_{mean} , e_{max} – Mean and maximum errors in pixels (left col.) and normalized in % of the diameter of the FOV (right col.)

IMAGE	$k_2 \times 10^{-4}$	$k_3 \times 10^{-6}$	$k_4 \times 10^{-8}$	$k_5 \times 10^{-11}$	Cx	Cy	e_{mean}		e_{max}	
							pixels	% FOV	pixels	% FOV
A0	5.36	1.42	2.46	6.54	190.2	118.9	1.33	0.30	3.70	0.84
A5	3.12	1.92	2.69	6.18	187.7	117.5	1.52	0.34	4.73	1.07
A10	5.59	1.09	2.32	6.28	188.5	121.0	0.94	0.21	3.68	0.83
B0	3.53	1.89	2.61	5.60	190.2	122.7	1.59	0.36	3.20	0.72
B5	4.44	2.04	2.68	5.68	186.4	123.8	1.90	0.43	5.59	1.26
B10	5.08	1.94	2.50	5.25	184.9	121.9	1.80	0.41	4.98	1.13
B0	5.99	2.58	3.29	6.79	190.5	125.6	1.67	0.38	7.15	1.62
B5	3.52	2.21	3.08	6.77	187.8	123.7	2.00	0.45	4.13	0.93
B10	3.14	2.03	3.02	7.02	186.6	125.3	1.74	0.39	6.20	1.4

Convergence was normally achieved in approximately 100 iterations (about 5 minutes computation time) for images acquired with endoscope positioned perpendicularly to the pattern. When the angle of acquisition increases, the number of iterations also increases, therefore the probability of reaching a local maximum becomes greater. We also observed that the optimisation algorithm was more easily trapped around a local maximum in the case of the circles pattern, than for both others. Table 1 gives the numerical values of the parameters computed by the algorithm for experiments in Figure 1. The values of k_4 and k_5 are in the same order of magnitude whatever the angle for each pattern confirming their little importance in the correction. A larger disparity exists between the values of k_2 and k_3 for the 3 patterns at same angles. The comparison of the values of normalized errors obtained for all images allows to evaluate more exactly the influence of the pattern type and of the inclination angle. For each of the 3 images acquired with an angular position up to 10° , the inclination does not have a significant influence on the mean errors e_{mean} (0.21 to 0.34% for A, 0.36 to 0.43% for B, 0.38 to 0.45% for C). The values of e_{mean} increase from A to B to C and comparing for respective angular positions, globally of about 30 to 60%. The values of maximal errors e_{max} are systematically 2 to 4 times greater than their corresponding mean errors values. However, all the values obtained for e_{mean} are fully acceptable since the maximal mean normalized error of 0.45% (obtained for the grey level pattern with inclination) is comparable to other referenced results [3]. Consequently, a fully automated correction-calibration procedure of a video-endoscope maintained roughly perpendicular and using a grey level pattern can be performed with a fully acceptable final error. The main advantage of the method over others [1,3,4] is its simplicity; no specifically precise pattern geometry is needed and the endoscope can be held with the hand.

4. CONCLUSIONS

The method here proposed is easy to apply and flexible

since radial distortion correction parameters can be determined in few minutes using a simple good contrasted grey level pattern acquired with the endoscope roughly perpendicular to it. Results were obtained with final errors comparable to those given by other methods necessitating specific calibration grid and positioning. Further tests are conducted in order to obtain and compare more statistic results.

5. ACKNOWLEDGMENTS

The authors would like to thank the financial supports from the CONACYT and the Ligue Contre le Cancer.

6. REFERENCES

- [1] R. Shahidi, M.R. Bax, C.R. Maurer, J.A. Jhonson, E.P. Wilkinson, B. Wang, J.B. West, M.J. Citardi, K.H. Manwaring, and R. Khadem, "Implementation, calibration and accuracy testing of image-enhanced endoscopy system," *IEEE Trans. Med. Imaging*, Vol.11, pp. 1524-1535, 2002.
- [2] H. Tian, T. Srikanthan, K.V. Asari, and S.K. Lam, "Study on the effect of object to camera distance on polynomial expansion coefficients in barrel distortion correction," in *Fifth IEEE Southwest symposium on Image Analysis and Interpretation SSIAP'02*, 2002.
- [3] J.P. Helferty, C. Zhang, G. McLennan, and W.E. Higgins, "Videoendoscopic distortion correction and its application to virtual guidance of endoscopy," *IEEE Trans. Med. Imaging*, Vol.20, pp. 605-617, 2001.
- [4] H.S. Sawhney, and R. Kumar, "True multi-image alignment and its application to mosaicing and lens distortion correction," *IEEE Trans. Pattern Anal. Machine Intell.*, Vol.18, pp. 235-243, 1999.
- [5] K.V. Asari, S. kumar, and D. Radhakrishnan, "A new approach for nonlinear distortion correction in endoscopic images based on least squares method," *IEEE Trans. Med. Imaging*, Vol.18, pp. 345-354, 1999.
- [6] W.E. Smith, N. Vakil, and A. Maislin, "Correction of distortion in endoscope images," *IEEE Trans. Med. Imaging*, Vol.11, pp. 117-122, 1992.